SECRETION IN DISSOCIATED HUMAN PULMONARY MAST CELLS

Evidence for Solubilization of Granule Contents before Discharge

JOHN P. CAULFIELD, ROBERT A. LEWIS, ANN HEIN, and K. FRANK AUSTEN

From the Departments of Pathology and Medicine, Harvard Medical School, and the Robert B. Brigham Division of the Affiliated Hospitals Center, Inc., Boston, Massachusetts 02115

ABSTRACT

Mast cells were enzymatically dissociated from human lung fragments that had been sensitized with serum from humans allergic to ragweed and were enriched by isopyknic and velocity gradient sedimentation. Electron microscope examination showed that the mast cells were well preserved at the end of the dissociation and isolation and that the majority of their secretory granules contained crystalline structures. These structures exhibited three patterns—scrolls, gratings, and lattices—which all could be found in the same granule. The period of crystalline structures was found to be bimodal, with maxima at 150 and 75 Å. Both periods were observed in gratings that had been tilted and in scrolls that had been cut obliquely, indicating that the various gross patterns are composed of the same basic substructure. After the mast cells were stimulated by rabbit anti-human IgE to release histamine, the contents of the granule were transformed from a crystalline to an amorphous state, and only granules with amorphous contents were seen discharging from the cell. Clusters of intermediate filaments were present around the granules with amorphous contents, both deep in the cytoplasm and discharging at the cell surface. Discharge occurred both by fusion of granule membranes with the plasma membrane and by fusion of granule membranes with other granule membranes that ultimately were continuous with the plasma membrane. After discharge, the granule residue was fibrillar. Cells challenged with anti-human IgE in calcium-free medium neither released histamine nor demonstrated morphologic changes in their granules. We conclude that the crystalline state represents a storage form for materials that are solubilized before fusion of the granule membrane with the plasma membrane and discharge.

Tissue mast cells mediate immediate IgE-dependent hypersensitivity reactions through the release of a variety of substances stored in their granules. Detailed morphologic studies of the secretory response of mast cells have, in general, been conducted with cells harvested by lavage from the peritoneal cavities of rodents. These cells, which can be obtained in numbers sufficient for study of purified populations, contain amorphous granules that do not permit ultrastructural analysis of early

phases of solubilization (29, 42). Human tissue mast cells exhibit a well-developed crystalline structure (11, 13, 21, 29, 44, 45) and afford the opportunity to examine the effect of IgE-dependent activation on this aspect of granule morphology. Furthermore, populations of dispersed human lung mast cells concentrated by sedimentation techniques (38) are suitable both in number of cells and in relative purity for a time-dependent ultrastructural analysis of the events following IgE-dependent activation.

MATERIALS AND METHODS

Chymopapain, collagenase type II, deoxyribonuclease type I (Worthington Biochemical Corp., Freehold, N. J.); elastase type I, atropine sulfate (Sigma Chemical Co., St. Louis, Mo.); B grade pronase (Calbiochem-Behring Corp., American Hoechst Corp., San Diego, Calif.); gelatin (Difco Laboratories, Detroit, Mich.); histamine acid phosphate (Mann Research Labs, Inc., New York); minimal essential medium (MEM) (Grand Island Biological Co., Grand Island, N. Y.); and metrizamide (Accurate Chemical Co., Hicksville, N. Y.) were purchased from the manufacturers. Hartley strain guinea pigs weighing 250–350 g were purchased from Charles River Farms, Wilmington, Mass. Rabbit anti-human IgE, directed against purified Shackford IgE myeloma (35), was heat-inactivated at 56°C for 30 min, precipitated in 40% ammonium sulfate, and subjected to immunoabsorption with IgE-free normal human serum coupled to Sepharose 4B by the cyanogen bromide method (1). The absorbed rabbit anti-IgE gave no precipitin lines upon immunoelectrophoresis with normal human serum but demonstrated anti-IgE activity by the line of identity obtained by radioimmunodiffusion against normal human serum and the IgE myeloma protein (25).

Dispersion and Enrichment of Human Lung Mast Cells

Grossly normal lung tissue weighing 25–100 g, obtained during surgery for carcinoma, was dissected free of blood vessels, major airways, and pleura and then finely fragmented. These fragments were washed and incubated for 12–15 h at 25°C in MEM, pH 7.4, containing 1 mM EDTA and serum from humans allergic to ragweed at a final dilution of 1:5. The incubation temperature was increased to 37°C during the final hour. The lung fragments were then washed three times in calcium-free Tyrode's buffer. Lung cells were dispersed by stirring the fragments gently at room temperature in Tyrode's buffer that contained pronase (2 mg/ml) and chymopapain (0.5 mg/ml); 1 ml of dispersion solution per g of lung tissue was used. After 30 min, freed cells were separated by sieving through nylon bolting cloth with a pore size of 160 μm (Tetko Inc., Elmsford, N. Y.) and were washed by sedimentation at 100 *g* for 5 min at 25°C in Tyrode's buffer that contained gelatin (1 mg/ml) and deoxyribonuclease (0.01 mg/ml) and that lacked calcium ions (TGD). The undigested lung was transferred to another portion of the same dispersion mixture, and a second 30-min incubation was carried out, after which the freed cells were harvested. The remaining undigested lung was then transferred to Tyrode's buffer that contained gelatin (1 mg/ml), collagenase (1 mg/ml), elastase (10 U/ml), and deoxyribonuclease (0.01 mg/ml) for a further 30-min incubation with cell collection; this step was then repeated. The four samples of washed, dispersed cells were pooled, washed, and resuspended in TGD (17, 33, 38).

2-ml portions of lung cells suspended in TGD were layered over each of 50–100 2-ml volumes of 23.5% (wt/vol) metrizamide in TGD and centrifuged at 600 *g* for 15 min at 25°C. The mast cell-enriched fraction was aspirated from the buffer-metrizamide interface of each tube and washed by sedimentation at 100 *g* for 5 min at 25°C. 5×10^7–3×10^8 cells from the preceding sedimentation were suspended in TGD, divided into 3–6 4-ml samples, and layered over an equal number of 35-ml linear gradients of 3–9% metrizamide in TGD. The gradients were centrifuged at 55 *g* for 12 min at 25°C. Cells were recovered in 4-ml fractions by sequential aspirations from the top. The purity of mast cell-enriched fractions from four separate lungs (38) ranged from 15 to 40%, as assessed in wet preparations stained with 0.1% toluidine blue in ethanol.

The mast cell-enriched suspension in Tyrode's buffer was apportioned into plastic tubes at concentrations of 1×10^6 mast cells/ml and preincubated for 5 min at 37°C. In four experiments, rabbit anti-human IgE was added at a final concentration of 1:25 to 12 replicate tubes, and triplicates were incubated for 0, 1, 3, or 5 min at 37°C. Additional triplicate tubes were incubated for 0 and 5 min in buffer alone. At each time point, the reaction in a single tube was terminated for transmission electron microscopy by the addition of an equal volume of fixative as described below. Duplicate reactions to be assayed for histamine were terminated by the addition of three volumes of ice-cold, calcium-free Tyrode's buffer. The cells were sedimented by centrifugation at 100 *g* for 5 min at 4°C, and the supernates were separated by decanting.

Residual histamine was extracted from the cell pellets by sequentially freezing and thawing them six times in 1 ml Tyrode's buffer. The histamine from each supernate and residual cell extract was separately quantitated by bioassay with the guinea pig ileum (8). The net percent of histamine release was calculated as [(stimulated release − unstimulated release)/(stimulated release + residual − unstimulated release)] × 100 and was then converted to the percent of net maximal histamine release for each experiment.

Preparation for Microscopy

Portions of intact lungs were fixed by the injection of 2–3 ml of cold (4°C) Karnovsky's aldehyde fixative (26) into the parenchyma. After 5 min, blocks were dissected from the lung, and aldehyde fixation was continued for an additional 20 min in vials. The blocks were then postfixed in acetate Veronal-buffered OsO_4 for 90 min at 4°C and stained in block in uranyl acetate for 2 h at 25°C (12). 1×10^6 dissociated mast cells were fixed in suspension at 4°C by the addition of an equal volume of Karnovsky's aldehyde fixative (26) that contained 1% formaldehyde and 3% glutaraldehyde in 0.1 M cacodylate buffer, pH 7.4, without calcium. After 15 min, the cells were pelleted in a Beckman Microfuge B (Beckman Instruments, Inc., Spinco Div., Palo Alto, Calif.) (2). The pellets were removed from the tubes, postfixed, and stained in block as described above. Dehydration and Epon embedding of both tissue and pellets were routine. Cells were also fixed in 2% glutaraldehyde and 0.2% tannic acid in 0.1 M cacodylate buffer, pH 7.2, for 1 h at 4°C, with multiple changes of the fixative, postfixed with OsO_4 for 1 h at 4°C, and stained in block as described above (3).

Microscopy

Thick sections (0.2 μm) of both tissue and pellets were cut

with glass knives and stained with azure II-methylene blue in sodium tetraborate. Pellets were cut from top to bottom, i.e., in the plane of the long axis of the centrifuge tube, to evaluate the distribution of the cell populations. Thin sections with silver-gray interference colors were cut with a diamond knife, picked up on Formvar-carbon-coated grids, stained on grid for 4 min in uranyl acetate and 1 min in lead citrate (41), and examined in a JEOL 100C electron microscope operating at 60 or 80 kV. The microscope was calibrated with grating 1002 from Ernest F. Fullman, Inc., Schenectedy, N. Y.

RESULTS

Human mast cells subjected to aldehyde fixation for 10–15 min at 4°C are well preserved, whereas fixation overnight or at 25°C results in extraction of the cytoplasm and the granule matrix. Tannic acid fixation accentuates the intermediate filaments (3). Aldehyde- and ferrocyanide-reduced osmium primary fixation (20) does not improve the morphology. Intact mast cells are located primarily in the lower third of the pellet, macrophages and various epithelial cells in the middle, and dead cells and cell fragments at the top. The mast cells in the pellet resemble the elongated cells seen *in situ* in freshly fixed lung, except that the dispersed isolated mast cells are round.

Unstimulated Cells

Mast cells have folds, 1–2 μm in length, distributed over their surfaces in patches (Fig. 1). A few cells have no surface folds. These folds are also seen in vacuoles in the cytoplasm just beneath the cell surface (Fig. 1). The cytoplasm is dominated by the secretory granules (see below). There are also many intermediate filaments, which average 83 Å (n = 100) in diameter and are located in the perinuclear region (Fig. 2). A few thin filaments are present in the surface folds and under the plasma membrane, but they usually appear to be disorganized. The nucleus is eccentric, with the Golgi apparatus nearby. A few mitochondria, the centriole, and microtubules are located mainly in the central portion of the cell.

The secretory granules are surrounded by a perigranular membrane (Fig. 2) that is often difficult to visualize. The contents of the granules have a variegated appearance but can be divided into two types–crystalline and amorphous (Fig. 2). Crystalline contents exhibit any of three basic patterns: (*a*) scrolls or whorls, which are the hallmark of this cell and which are seen in 60–80% of the granules (Figs. 1–3); (*b*) gratings, which are parallel, electron-dense lines separated by lucent areas and which are present in 10–30% of the granules (Fig. 4); and (*c*) lattices, which consist of two sets of parallel, electron-dense lines running in different directions, overlying one another, and which are observed in only 2% of the granules (Fig. 5). All three patterns may be seen in the same granule (Fig. 5). The scroll pattern may be formed by concentric circles (Fig. 3 *a*) or by one or more layers coiled inside one another (Fig. 3 *a*). When cut along their long axis, the scrolls appear as two fasciae of four or five electron-dense lines separated from one another by electron lucent spaces of approximately the same width as one of the fasciae (Fig. 3 *b*). Measurements of the period, i.e., the distance from the beginning of one electron-dense line to the beginning of the next, of all three types of crystalline structure fall into a bimodal distribution, with maxima at ~75 and 150 Å (Fig. 6). To test whether these two periods exist in the same crystalline structure, specimens were tilted in the microscope over a range of ±35° with a eucentric goniometer. Crystals with grating patterns show 150 and 75 Å periods at different tilt angles (Fig. 4). These two spacings are oriented in different directions and, therefore, must occur in the same crystal. In addition, scrolls cut obliquely have a short period oriented in a direction different from that of the long period (Fig. 3 *b*).

The second major type of granule content is amorphous (Fig. 2), even upon examination at high magnification (50,000) and tilting of the section. Granules with amorphous contents make up only 5–10% of the total and are larger, averaging 1 μm in diameter (n = 50) than the crystalline granules, which average 0.5 μm in diameter (n = 50) (Figs. 1 and 2). In addition, these granules often have a saccule composed of a double membrane ring, which extends partially or completely around the outside of the granule membrane (Fig. 2). This saccule contains a cisternal space and is flattened along the contour of the granule (Fig. 2).

Anti-IgE Stimulated Secretion

Significant alterations are seen in the crystalline content morphology during the first 3 min after stimulation. With IgE-dependent stimulation of histamine release (Fig. 7), the 1- and 3-min specimens show a general breakdown of the structure of the crystalline matrix, with the appearance of electron-dense clumps in the center of the scrolls and throughout the matrix of those granules with a lattice or grating pattern (Fig. 8). In some cells, there is a further loss of crystalline structure, and

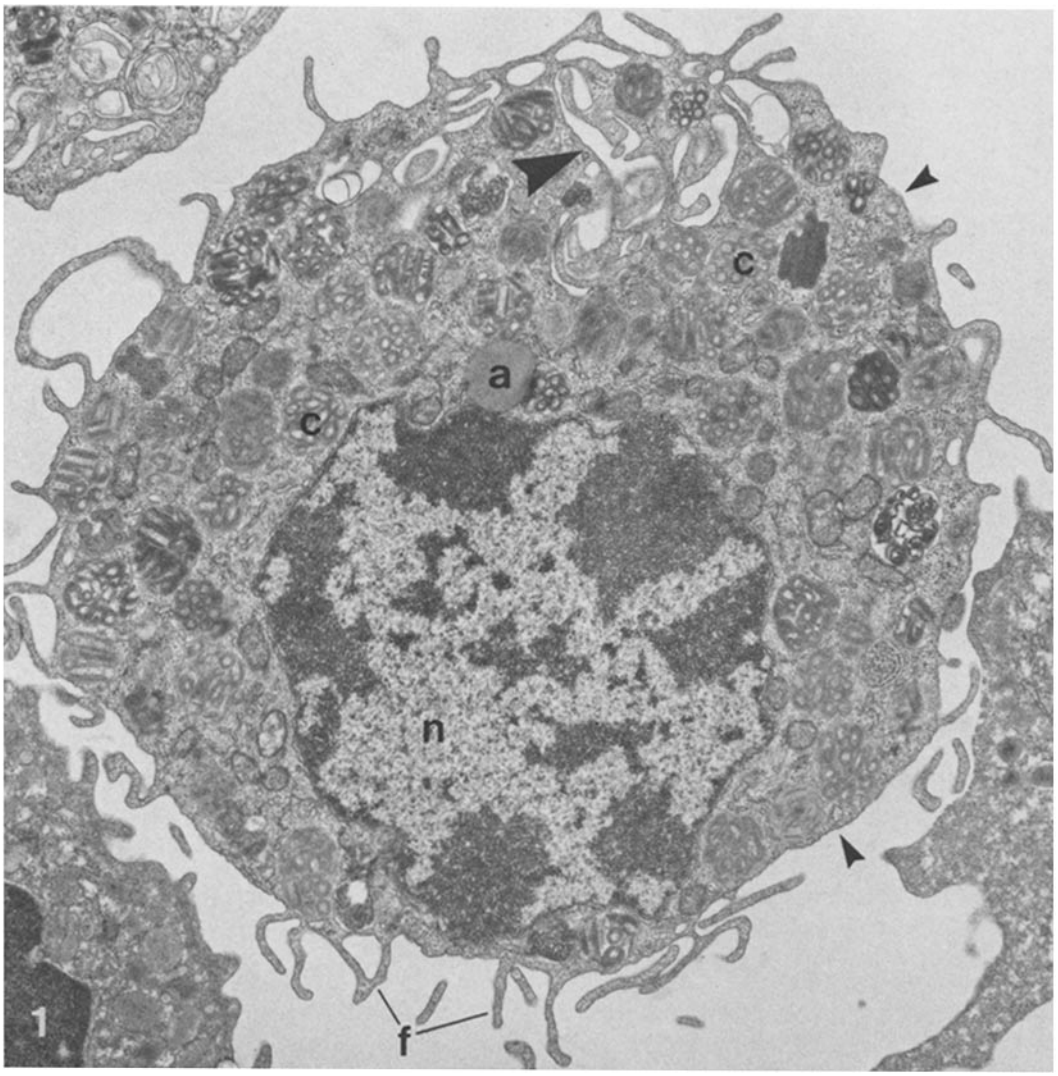

FIGURE 1 Low power view of a mast cell dissociated from human lung. Surface folds (*f*) are absent from some areas (small arrowheads). Some folds appear to have been endocytosed (large arrowhead). The cytoplasm is dominated by the secretory granules, most of which contain crystalline scrolls (*c*). One appears to have amorphous contents (*a*). Nucleus (*n*). The tissue was fixed in aldehydes at 4°C, postfixed in OsO_4, and stained in block with uranyl acetate and on grid with uranyl acetate and lead citrate. × 13,000.

electron-dense clumps appear to form a reticulum (Fig. 9). Less commonly, in other cells, the entire center of the granule is seen as an amorphous, electron-dense mass (Fig. 10). The net result of these changes in granules with crystalline contents is that there is an increase in the number of granules with amorphous contents in the cell (Fig. 11), some of which have perigranular saccular structures associated with them (Figs. 11 and 12). The membrane of many of these granules appears to be in contact with intermediate filaments (Figs. 11 and 12). In tangential section, the filaments surround the granule in clusters that often are arranged in parallel (Figs. 11, 12*c*, and 12*d*). In normal section, the filaments appear to touch the perigranular membrane (Figs. 12*a* and 12*b*).

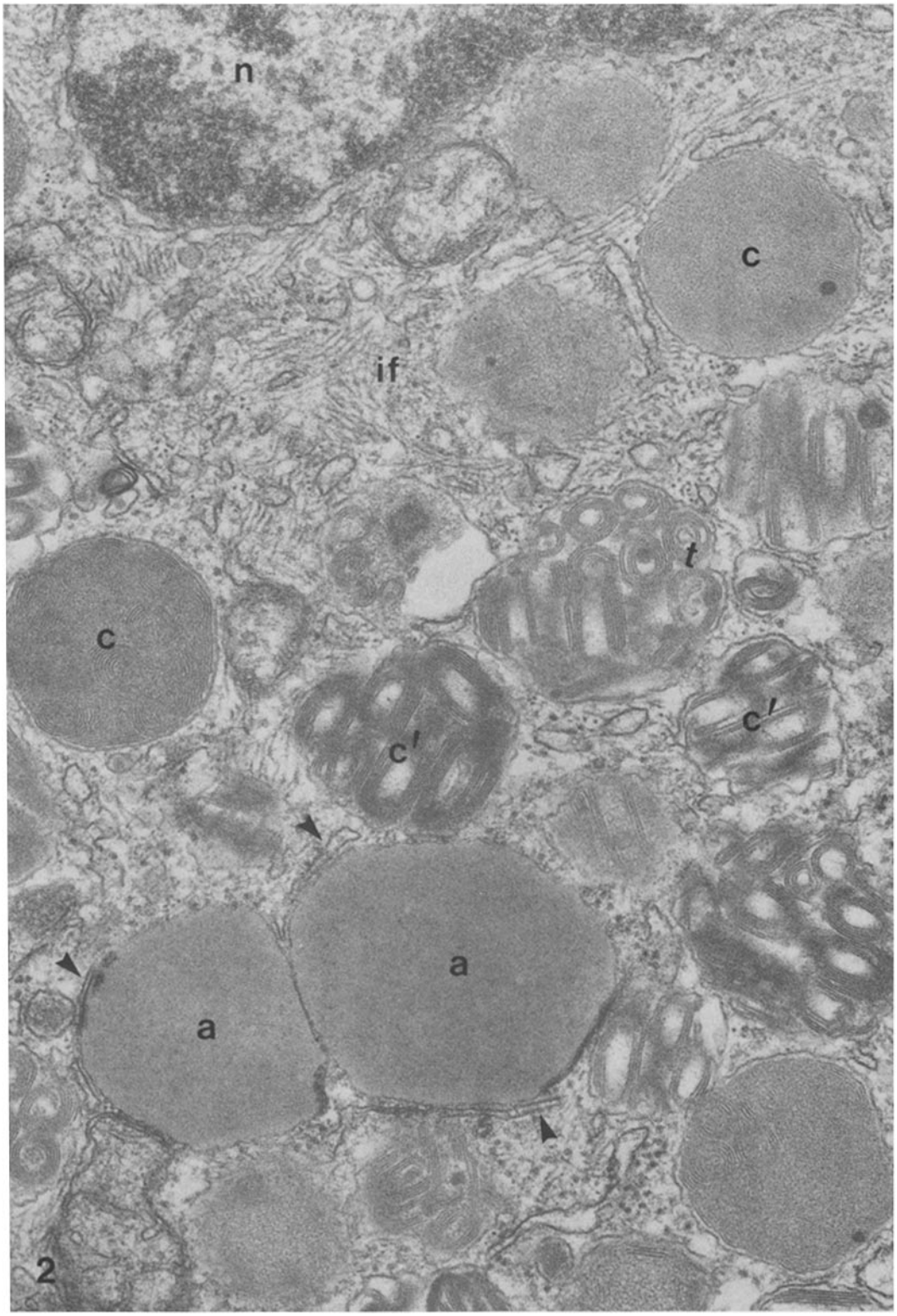

FIGURE 2 Cytoplasm of a dissociated human lung mast cell. Most of the granules contain crystalline patterns consisting of scrolls and parallel lines formed by scrolls cut along the long axis. The granules have either a dark (*c*) or a light (*c′*) matrix behind the crystalline pattern. At the bottom of the micrograph are two granules with amorphous contents (*a*). Flattened saccules (arrowheads) appear against the granules, and prominent intermediate filaments (*if*) are seen near the nucleus (*n*). The specimen preparation was as described in Fig. 1. × 51,000.

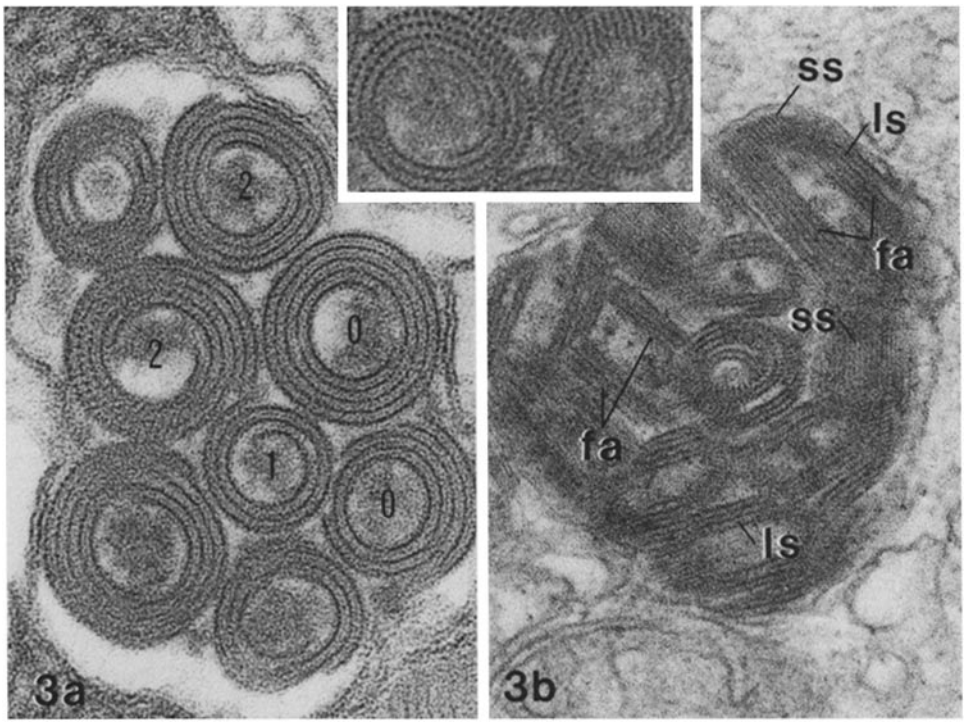

FIGURE 3 Crystalline granules from unstimulated cells. (*a*) The scrolls consist of concentric layers (*0*) or of one or more layers coiled within one another (*1* and *2*). The *inset* shows that the layers have a beaded structure and that there is a radial spacing in addition to the concentric one in the scroll on the right. *b* shows both 75-Å (*ss*) and 150-Å (*ls*) periods occurring in the same scrolls. Many scrolls cut along their long axis appear as fasciae (*fa*) of electron-dense lines separated by electron-lucent spaces. (*a*) × 192,000; (*b*) × 101,000; (*inset*) × 208,000.

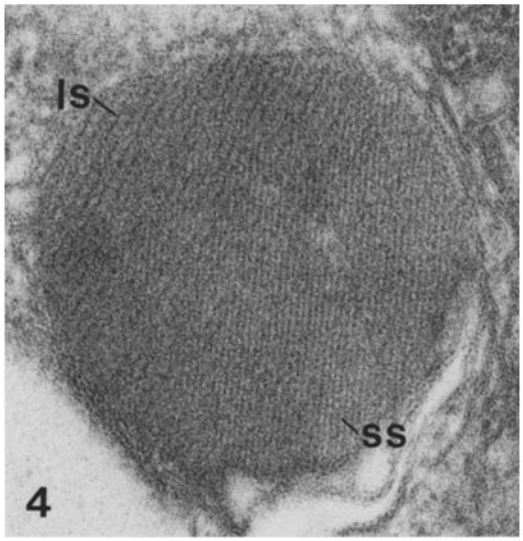

FIGURE 4 A crystalline granule containing both 150-Å (*ls*) and 75-Å (*ss*) spacing. This granule, when tilted, showed three 150-Å and two 75-Å spacings, all oriented along different axes. × 137,000.

Mast cells are seen discharging granules from the surface of the cell by 1 min after stimulation, and, by 3 min, this discharge is marked, with minimal further increase occurring after 5 min. Only granules with amorphous contents are seen discharging (Figs. 11 and 13). The granules discharge by fusing either with the plasma membrane (Figs. 11 and 13) or with other granule membranes to form deep channels or labyrinths composed of the interconnected membranes of discharged granules within the cell (Fig. 14). After discharge, the granule residue is fibrillar (Figs. 13 and 14). The granules have intermediate filaments associated with their perigranular membranes throughout exocytosis (Figs. 11 and 13). The surface membrane of cells containing labyrinths has more and longer extensions than the normal cell, and very few granules with crystalline contents are seen within the cytoplasm (Fig. 14). None of these changes is seen in cells challenged with anti-IgE in the absence of extracellular calcium; under these circumstances, there is no induced net histamine release.

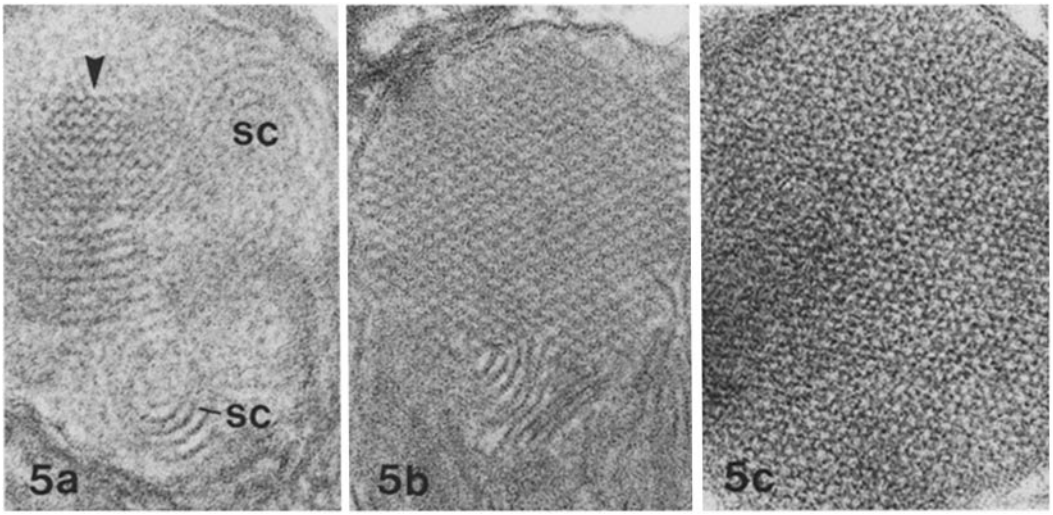

FIGURE 5 A variety of granules showing intersecting line or lattice patterns. (*a*) A herringbone pattern (arrowhead) in a granule that also contains a scroll (*sc*); (*b*) a typical lattice pattern; (*c*) a lattice pattern, usually seen in hexagonally packed crystals. (*a*) × 155,000; (*b*) × 78,000; (*c*) × 210,000.

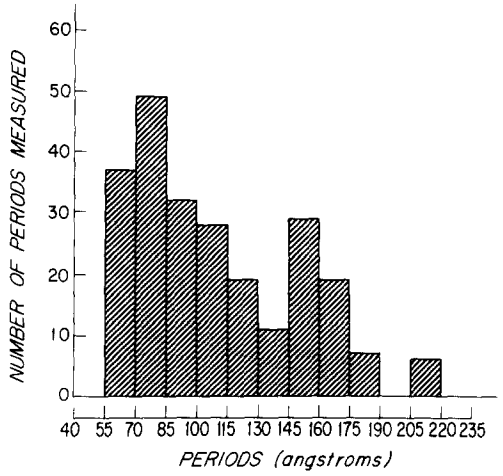

FIGURE 6 Histogram of the distribution of the measurements of the period, or repeat distances, in scrolls and gratings. The distribution is bimodal and is skewed around the maxima, which occur at ~75 and 150 Å. Lines were measured in 40 cells.

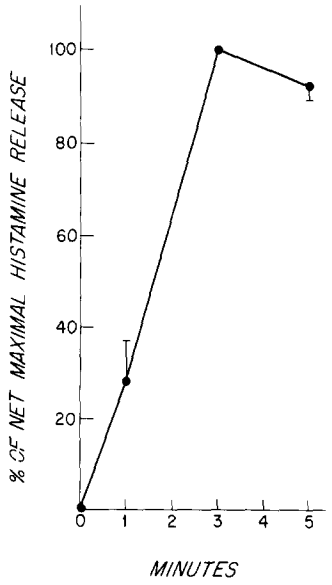

FIGURE 7 Time course of histamine release from immunologically activated human lung mast cells. In each of four experiments, duplicate portions were assayed for net percent of histamine release at each time point. Net maximal histamine release ranged from 11.0 to 19.5% at 3 min after challenge. This value for each experiment was set at 100%, and the control release at 0 time at 0%. On this basis, percent of histamine release at 1 and 5 min were calculated as percent of maximum release ± SEM (bars). Release from unstimulated cells ranged from 0.4 to 1.8%.

DISCUSSION

Mast cells dissociated from human lung are morphologically well preserved and resemble closely mast cells seen in intact human lung (7, 43), intestine (11, 29), corneal limbus (21), gingiva (45), and skin (6, 9, 13, 14, 18, 19, 27, 28, 44). Resting or unstimulated dispersed mast cells are characterized by granules with crystalline contents that contain three patterns—scrolls, gratings, and lattices—which can coexist within the same granule

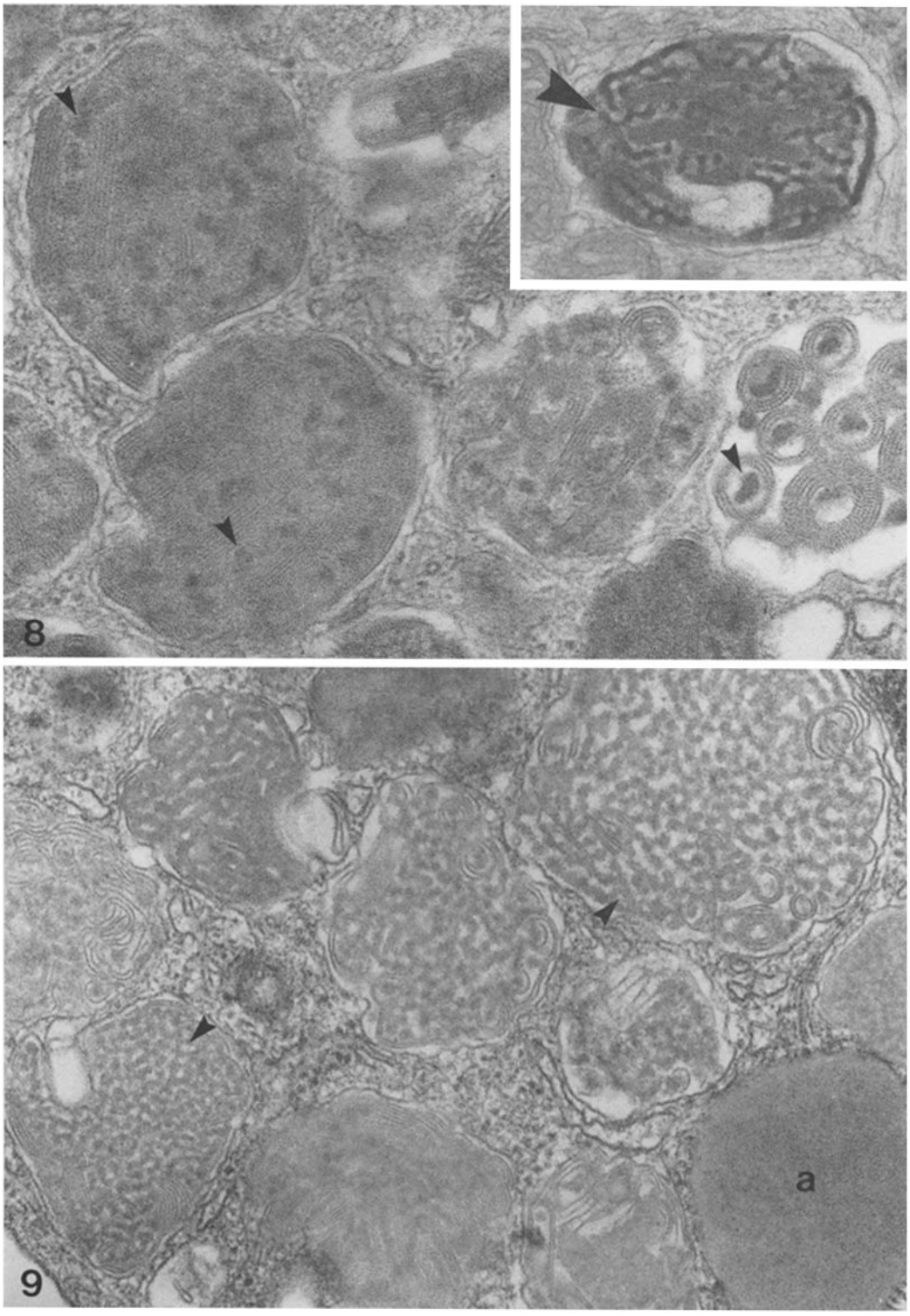

FIGURE 8 Crystalline granules from a mast cell 3 min after exposure to anti-IgE. Discrete electron-dense structures (arrowheads) are seen in granules with both light and dark background matrices. These structures seem to locate preferentially in the center of the scrolls. *Inset* shows continuity between electron-dense structures to form lines, some of which appear helical (arrowhead). Tissue preparation was as described in Fig. 1. × 74,000; (*inset*) × 72,000.

FIGURE 9 Granules from a mast cell 3 min after exposure to anti-IgE. The crystalline structure has largely been lost in most granules, and electron-dense material forms a reticular pattern (arrowheads). An amorphous granule (*a*) is seen at the lower right. Tissue preparation was as described in Fig. 1. × 68,000.

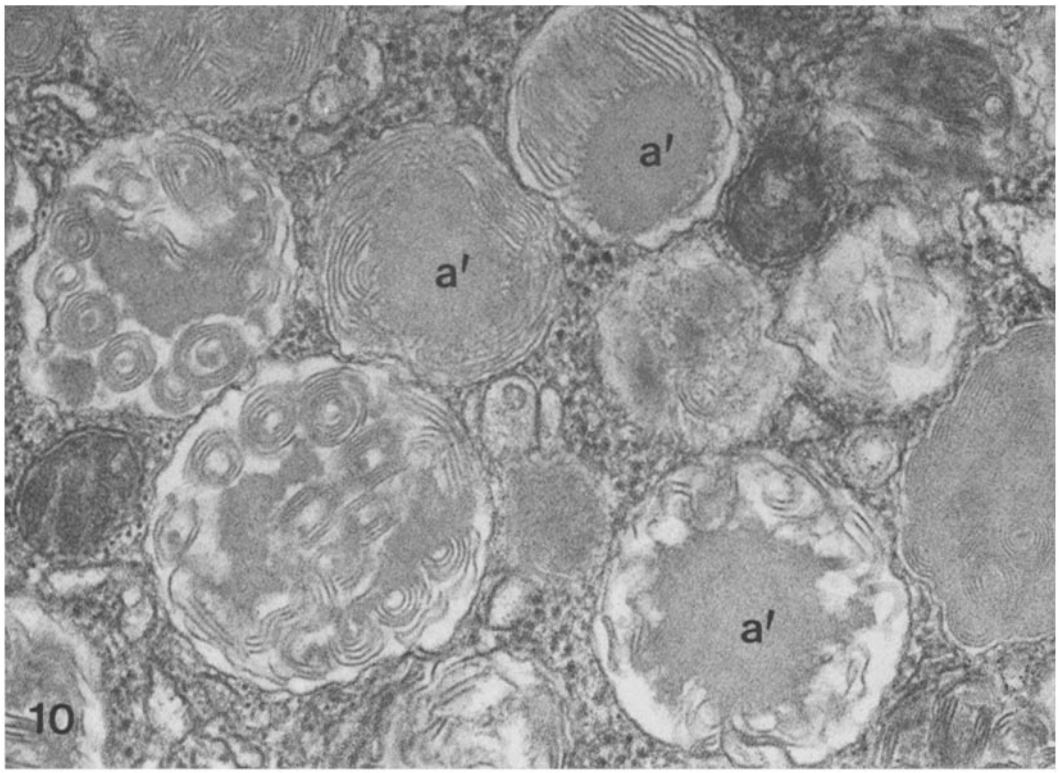

FIGURE 10 Granules from a mast cell 5 min after exposure to anti-IgE. Several granules contain a large amorphous mass (*a'*) forming in the center of the crystalline patterns. Tissue preparation as described in Fig. 1. × 72,000.

(11, 21, 29, 45). Other investigators have measured the periods or repeat distances in these structures in tissue mast cells and have described either two periods (11, 28) or a single period (9, 13, 14, 19, 21, 43, 45). These authors have not given a distribution for their measurements. Because of the bimodal distribution of the periods, and because two different periods can be seen in a single grating or in scrolls cut obliquely (11), we believe that there are two periods, which represent different views of the same basic crystalline structure, which, in turn, makes up all three patterns of crystals seen within the granule. The diversity in the absolute values of the reported periodicity measurements, i.e., 60–75 and 120–150 Å, is in all probability due to the variety of methods of fixation. The chemical nature of the crystalline structure is unknown; but because of the large size of the two periods, it is most likely proteinaceous.

In addition to the granules with crystalline contents, the unstimulated cell also contains a few granules with amorphous contents. These granules are distinct from the crystalline granules because they contain no internal structure, but they presumably contain the same material that is seen in the crystalline granules because transformation from crystalline to amorphous contents in the stimulated cell is observed. Their functional relevance in the resting mast cell is unclear. They might represent newly synthesized granules, analogous to condensing vacuoles in pancreatic acinar cells (22, 23), or they may be a population of granules that is available for more rapid discharge. The crystalline structure possibly represents a highly concentrated form of granule content, which would be in keeping with data obtained from isolated rat mast cell granules that indicate strong ionic interactions between heparin, histamine, and the cationic protein chymase (5, 30–32, 46). Ionic interactions between granule molecules have also been invoked to explain the condensation of proteins that occurs during protein synthe-

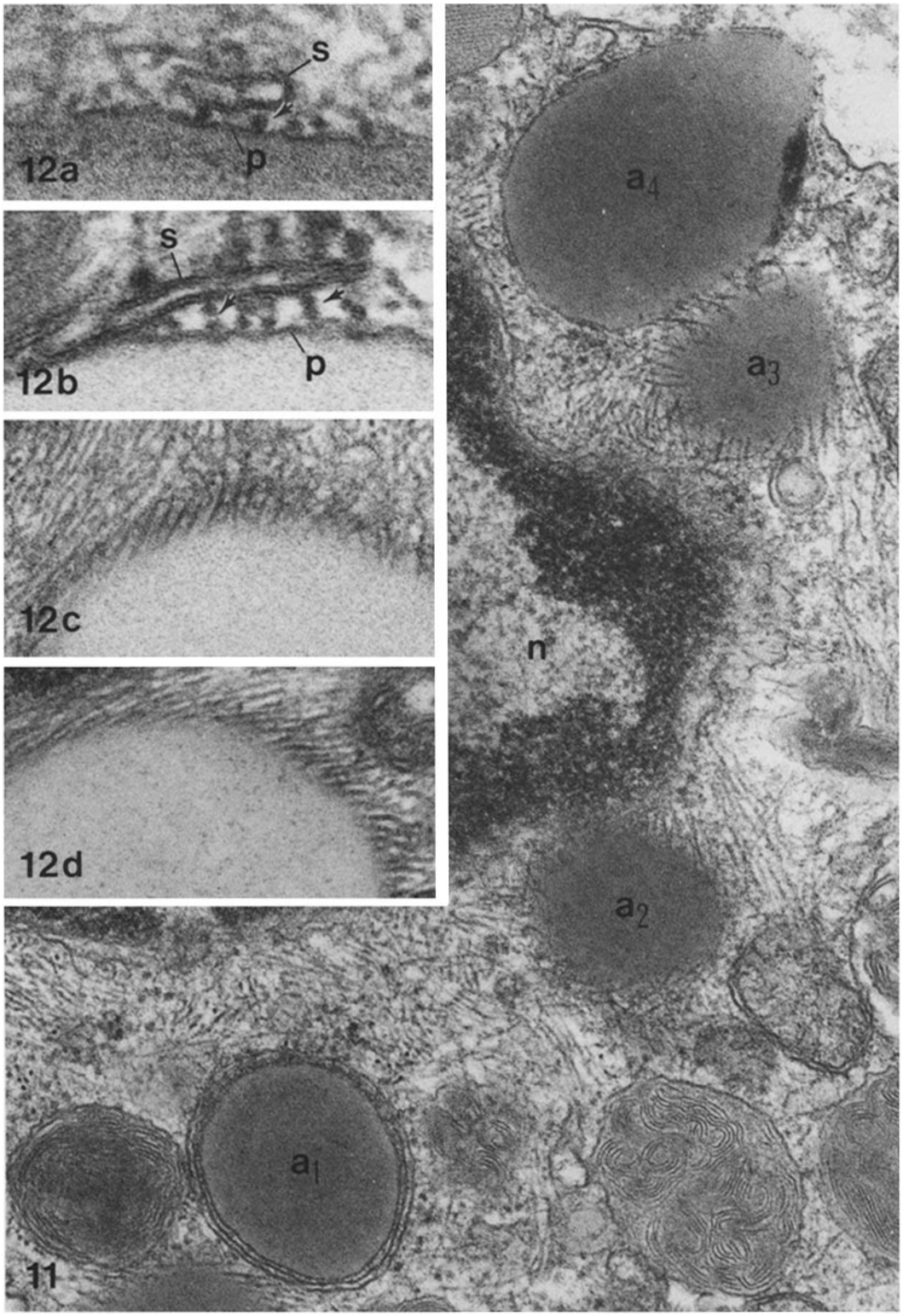
s
p
12a
s
p
12b
12c
12d
a4
a3
n
a2
a1
11

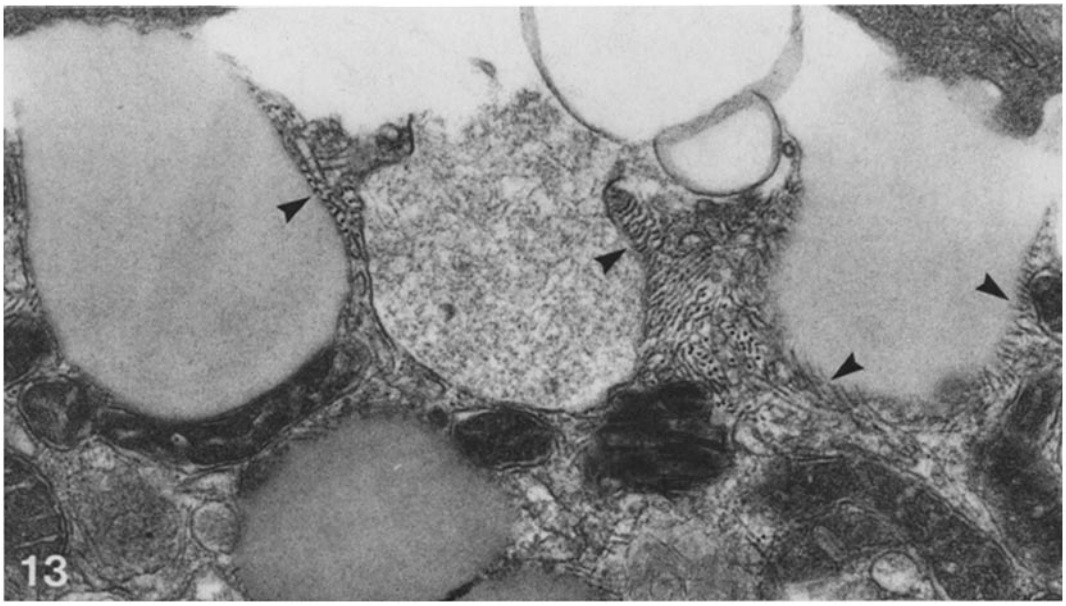

FIGURE 13 High power view of granules discharging from the surface of mast cell stimulated with anti-IgE 3 min before fixation. The granules on the right and left contain no crystalline structure. The residue of the granule in the center is fibrillar (see also Fig. 14). Intermediate filaments are seen around all three granules, particularly in the areas marked by arrowheads. Tissue preparation was as described in Fig. 1. × 49,000.

sis when the proteins move from the Golgi apparatus to the zymogen granules in the guinea pig pancreas (22, 23, 39, 40). Finally, the suggestion that the crystalline human mast cell granule contents are a storage form is supported by the transformation of these contents to the amorphous form before discharge.

Stimulated or activated mast cells are altered in three ways. Firstly, the crystalline contents become amorphous. Secondly, only the granules with amorphous contents discharge, leaving a fibrillar residue in the granule lumen. Thirdly, intermediate filaments cluster around the granules with amorphous contents whether they are located deep in the cytoplasm or are discharging from the cell surface. The transformation of the granule content from the crystalline to the amorphous state suggests that at least partial solubilization of the granule contents is occurring before discharge. Furthermore, the increase in diameter of the amorphous granules is consistent with the increase in osmotic pressure in the granule that would result from solubilization. Comparable observations have not been made in other secretory systems and

FIGURE 11 Mast cell stimulated with anti-IgE 3 min before fixation. Four granules with amorphous contents can be seen. One (a_1) is surrounded by a double membrane similar to the saccules shown in Fig. 2. Two others (a_2 and a_3) are surrounded by clusters of intermediate filaments. The fourth (a_4) is bulging from the cell surface, and the perigranular and plasma membranes are nearly fused. Nucleus (*n*). Tissue preparation was as described in Fig. 1. × 75,000.

FIGURE 12 High power views of intermediate filaments and granules with amorphous contents. *a* and *b* are normal sections showing that the filaments (arrows) are touching the perigranular membrane (*p*). In *b*, the filaments appear as pairs. In both *a* and *b*, the flattened saccules (*s*) also seem close to the filaments. In *c* and *d*, the filaments are cut along their long axis and are seen to approach the granule tangentially and in parallel. Tissue preparation in *a*, *b*, and *c* was as described in Fig. 1. Tissue in *d* was fixed in tannic acid and glutaraldehyde, postfixed in OsO_4, and stained in block in uranyl acetate and on grid with uranyl acetate and lead citrate. (*a*) × 205,000; (*b*) × 230,000; (*c*) × 78,000; (*d*) × 86,000.

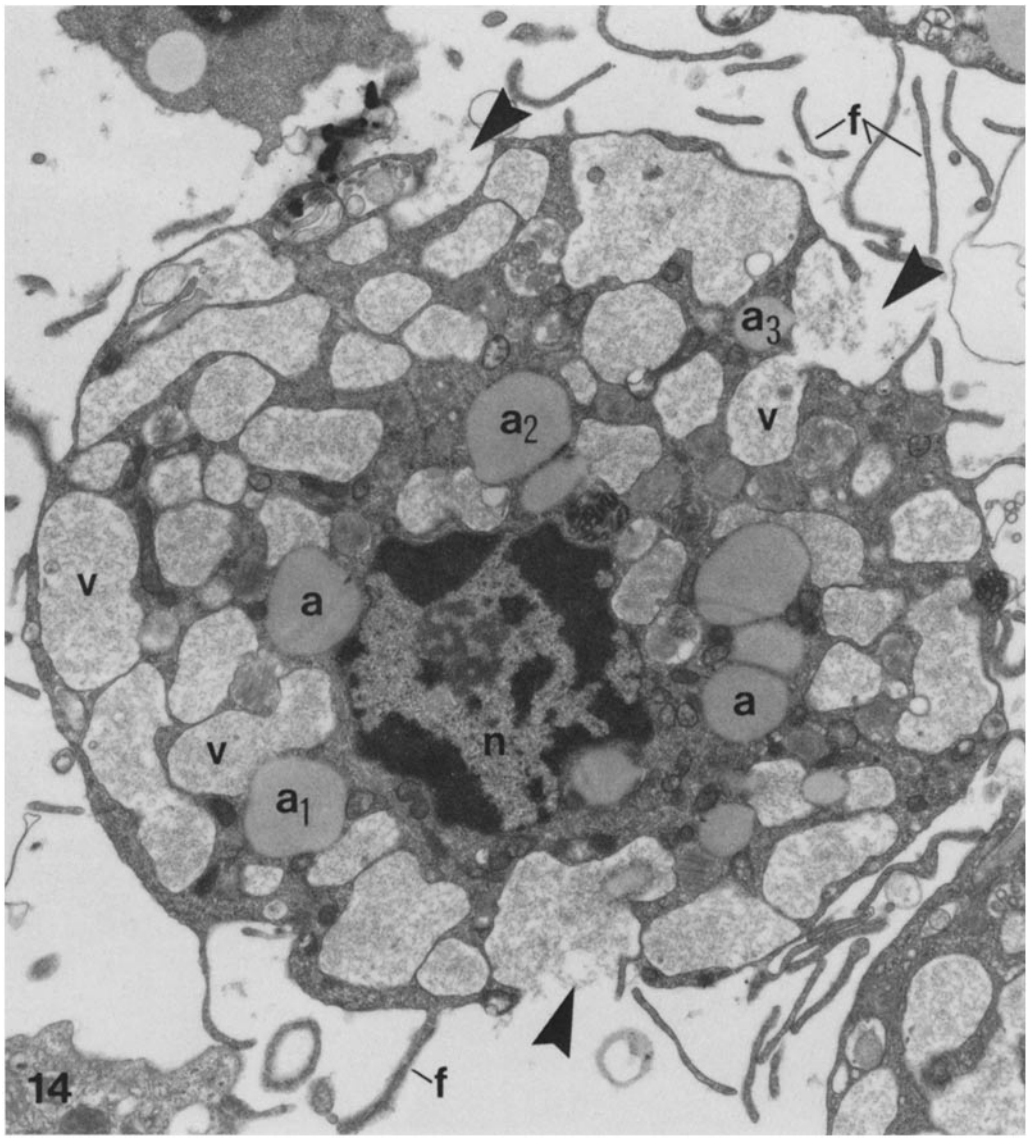

FIGURE 14 Mast cell 5 min after stimulation with anti-IgE. The surface folds (*f*) are much longer than in the unstimulated cell (see Fig. 1). The cytoplasm is filled by dilated vacuolar spaces (*v*) that communicate with the extracellular space in several places (large arrowheads). Most of the granules remaining in the cytoplasm have amorphous contents (*a*), and some of these (a_1, a_2, and a_3) appear to be about to discharge into the vacuolar spaces next to them. Nucleus (*n*). Tissue preparation was as described in Fig. 1. × 12,000.

are only possible here because of the crystalline nature of the granule content in the unstimulated mast cells. The mechanism of solubilization is not clear, but the lack of transformation in the absence of calcium suggests a role for that cation early in secretion.

Discharge or exocytosis establishes contact between the granule contents and the extracellular space (37). The morphology of discharge in the human lung mast cell is similar to that seen in most other stimulus-release types of cells (37), except that there is extensive fusion of granule membranes with one another to produce channels of granules connected with one another and to the

surface. This process also occurs in the rat mast cell (29, 42). After discharge, granule content molecules presumably dissociate from one another by ion exchange with the surrounding medium. This mechanism has been suggested for rat mast cells. In this case, histamine and heparin, measured after salt solubilization of discharged granules, appear in the medium in stoichiometric ratios after immunologic challenge (47). The fibrillar residues seen at the end of discharge presumably are granule contents that are partially or completely insoluble in the experimental medium. The elongation of the surface folds seen after discharge is similar to that seen in the rat mast cell (10).

The intermediate filaments are seen in contact with the membrane of amorphous granules located both deep in the cytoplasm and at the cell surface where discharge is occurring. The fact that intermediate filaments are seen around the discharging granules is particularly important because these filaments are ordinarily located in the central perinuclear regions of the cell, and because the subcortical portion of the cell is characteristically occupied by a feltwork of disrupted thin filaments (15, 16). This translocation of the intermediate filaments suggests that they have become associated with the granule membrane and have been moved to the surface along with the granule, perhaps through an interaction between the subcortical thin filaments and the perigranular intermediate filaments. Intermediate filaments have also been associated with the movement of pigment granules in melanocytes in human (24) and frog skin (34).

Most of the previous studies on secretion in human mast cells have been conducted on skin nodules from biopsy samples of patients with urticaria pigmentosa (14, 18, 27). These nodules, which contain large numbers of mast cells that degranulate upon tactile stimulation, were removed by punch biopsy after stimulation and processed for microscopy. Other studies have been performed on skin obtained by biopsy from a patient with diffuse mastocytosis (36), on nasal and bronchial biopsy cells (43), and on isolated adenoid cells stimulated with calcium ionophore A23187 (4). Several of these analyses utilized primary OsO_4 fixation (14, 18, 36), or long periods (hours) of fixation in glutaraldehyde, both of which have resulted in cells with an extracted and distorted cytoplasm. In unstimulated cells, all authors agree that most of the granules are crystalline but regard the amorphous granules as lipid droplets (4, 11, 18, 43). In stimulated cells, several authors noted a loss of crystalline structure (18, 27, 43), but some regard this as regranulation (27) rather than transformation. Others noticed filaments around the granules but generally considered them to be microfilaments (4, 43). Granules with crystalline contents seen outside the cell (18, 27, 43) are regarded as discharged, but no consideration is given to the possibility that they could result from the punch biopsy technique. One group recognized discharging granules with amorphous contents but did not relate them to the crystalline granules (4). Finally, labyrinth formation was generally noted.

The authors would like to thank Dr. Stephen Harrison, Dr. Gabriel Godman, Dr. Sally Zigmond, and Dr. Mark Mooseker for their helpful discussions during the course of this work and Ms. Judith Litvin for her excellent technical assistance. This work was supported, in part, by grants AI-07722, AI-10356, RR-05669, HL-17382, HL-19777, and HL-21089 from the National Institutes of Health and by a grant from The New England Peabody Home for Crippled Children.

Received for publication 7 November 1979.

REFERENCES

1. AXEN, R., J. PORATH, and S. ERNBACK. 1967. Chemical coupling of peptides and protein to polysaccharides by means of cyanogen halides. *Nature (Lond.)*. **214**:1302–1304.
2. BAINTON, D. F., and M. G. FARQUHAR. 1968. Differences in enzyme content of azurophil and specific granules of polymorphonuclear leukocytes. II. Cytochemistry and electron microscopy of bone marrow cells. *J. Cell Biol.* **39**:299–317.
3. BEGG, D. A., R. RODEWALD, and L. REBHUN. 1978. The visualization of actin filament polarity in thin sections. Evidence for the uniform polarity of membrane-associated filaments. *J. Cell. Biol.* **79**:846–852.
4. BEKRENDT, H., U. ROSENKRANZ, and W. SCHMUTZLER. 1978. Ultrastructure of isolated human mast cells during histamine release induced by ionophore A23187. *Int. Arch. Allergy Appl. Immunol.* **56**:188–192.
5. BERQVIST, U., G. SAMUELSSON, and B. UVNÄS. 1971. Chemical composition of basophil granules from isolated rat mast cells. *Acta Physiol. Scand.* **83**:362–372.
6. BOWYER, A. 1968. Observations on the granularity of mast cells in human skin. *Acta Dermato-Venereol.* **48**:574–577.
7. BRINKMAN, G. L. 1968. The mast cell in normal human bronchus and lung. *J. Ultrastruct. Res.* **23**:115–123.
8. BROCKLEHURST, W. E. 1960. The release of histamine and formation of slow reacting substance (SRS-A) during anaphylactic shock. *J. Physiol. (Lond.)* **151**:416–435.
9. BURNS, C. P., and J. C. HOAK. 1975. Freeze-etch studies of the granules of human mast cells and eosinophils. *J. Ultrastruct. Res.* **50**:143–149.
10. BURWEN, S. J., and B. H. SATIR. 1977. Plasma membrane folds on the mast cell surface and their relationship to secretory activity. *J. Cell Biol.* **74**:690–697.
11. DOBBINS, W. O., J. T. TOMASINI, and E. L. ROLLINS. 1969. Electron and light microscopic identification of the mast cell of the gastrointestinal tract. *Gastroenterology.* **56**:268–279.
12. FARQUHAR, M. D., and G. E. PALADE. 1965. Cell junctions in amphibian skin. *J. Cell Biol.* **26**:263–291.
13. FEDORKO, M. F., and J. G. HIRSCH. 1965. Crystalloid structures in granules of guinea pig basophils and human mast cells. *J. Cell Biol.* **26**:973–976.
14. FREEMAN, R. G. 1967. Diffuse urticaria pigmentosa. An ultrastructural study before and after whealing. *Am. J. Clin. Pathol.* **48**:187–199.
15. GODMAN, G. C., and A. F. MIRANDA. 1978. Cellular contractility and

the visible effects of cytochalasin. *In* Cytochalasins—Biochemical and Cell Biological Aspects. S. W. Tannenbaum, editor. Elsevier North-Holland, Inc., New York. 277–429.
16. GOLDMAN, R., and D. KNIPE. 1973. Functions of cytoplasmic fibers in non-muscle cell motility. *Cold Spring Harbor Symp. Quant. Biol.* **37:** 523–534.
17. GOULD, K. G., J. A. CLEMENTS, A. L. JONES, and J. M. FELTS. 1972. Dispersal of rabbit lung into individual viable cells: a new method for the study of lung metabolism. *Science (Wash. D.C.).* **178:**1209–1210.
18. HASHIMOTO, K., B. G. GROSS, and W. F. LEVER. 1966. An electron microscopic study of the degranulation of mast cell granules in urticaria pigmentosa. *J. Invest. Dermatol.* **46:**139–149.
19. HASHIMOTO, K., W. M. TARNOWSKI, and W. F. LEVER. 1967. Reifung und Degranulierung der Mastzellen in der menschlichen Haut. *Hautarzt.* **18:**318–324.
20. HASTY, D. L., and E. D. HAY. 1978. Freeze-fracture studies of the developing cell surface. II. Particle-free membrane blisters on glutaraldehyde-fixed corneal fibroblasts are artifacts. *J. Cell Biol.* **78:**756–768.
21. IWAMOTO, T., and G. K. SMELSER. 1965. Electron microscopic studies on the mast cells and blood and lymphatic capillaries of the human corneal limbus. *Invest. Ophthalmol.* **4:**815–834.
22. JAMIESON, J. D., and G. E. PALADE. 1967. Intracellular transport of secretory proteins in the pancreatic exocrine cell. II. Transport to condensing vacuoles and zymogen granules. *J. Cell Biol.* **34:**597–615.
23. JAMIESON, J. D., and G. E. PALADE. 1968. Intracellular transport of secretory proteins in the pancreatic exocrine cell. IV. Metabolic requirements. *J. Cell Biol.* **39:**589–603.
24. JIMBOW, K., and T. FITZPATRICK. 1975. Changes in distribution pattern of cytoplasmic filaments in human melanocytes during ultraviolet-mediated melanin pigmentation. The role of the 100-Å filaments in the elongation of melanocytic dendrites and in the movement and transfer of melanosomes. *J. Cell Biol.* **65:**481–488.
25. KALINER, M., R. P. ORANGE, and K. F. AUSTEN. 1972. Immunological release of histamine and slow reacting substances of anaphylaxis from human lung. IV. Enhancement by cholinergic and alpha adrenergic stimulation. *J. Exp. Med.* **136:**556–567.
26. KARNOVSKY, M. J. 1965. A formaldehyde-glutaraldehyde fixative of high osmalality for use in electron microscopy. *J. Cell Biol.* **27**(2, Pt. 2):137 *a* (Abstr.).
27. KOBAYASI, T., and G. ASBOE-HANSEN. 1969. Degranulation and regranulation of human mast cells. *Acta Dermato-. Venereol.* **49:**369–381.
28. KOBAYASI, T., K. MIDTGARD, and G. ASBOE-HANSEN. 1968. Ultrastructure of human mast cell granules. *J. Ultrastruct. Res.* **23:**153–165.
29. LAGUNOFF, D. 1972. Contributions of electron microscopy to the study of mast cells. *J. Invest. Dermatol.* **58:**296–311.
30. LANGUNOFF, D. 1974. Analysis of dye binding sites in mast cell granules. *Biochemistry.* **13:**3982–3986.
31. LAGUNOFF, D., M. T. PHILLIPS, O. A. ISERI, and E. P. BENDITT. 1964. Isolation and preliminary characterization of rat mast cell granules. *Lab. Invest.* **13:**1331–1344.
32. LAGUNOFF, D., and P. PRITZL. 1976. Characterization of rat mast cell granule proteins. *Arch. Biochem. Biophys.* **173:**554–563.
33. LEWIS, R. A., S. I. WASSERMAN, E. J. GOETZL, and K. F. AUSTEN. 1974. Formation of slow-reacting substance of anaphylaxis in human lung tissue and cells before release. *J. Exp. Med.* **140:**1133–1146.
34. MOELLMAN, G., J. MCGUIRE, and A. LERNER. 1973. Intracellular dynamics and the fine structure of melanocytes. With special reference to the effects of MSH and cyclic AMP on microtubules and 10 nm filaments. *Yale J. Biol. Med.* **46:**337–360.
35. OGAWA, M., S. KOCHWA, C. SMITH, K. ISHIZAKA, and O. R. MCINTYRE. 1969. Clinical aspects of IgE myeloma. *N. Engl. J. Med.* **281:**1217–1220.
36. ORFANOS, C., and G. STUTTGEN. 1962. Elektronenmikroskopische Beobachtungen zur Mastzelldegranulation bei der diffusen Mastocytose des Menschen. *Arch. Klin. Exp. Dermatol.* **214:**521–548.
37. PALADE, G. E. 1975. Intracellular aspects of the process of protein secretion. *Science (Wash. D. C.).* **189:**347–358.
38. PATERSON, N. A. M., S. I. WASSERMAN, J. W. SAID, and K. F. AUSTEN. 1976. Release of chemical mediators from partially purified human lung mast cells. *J. Immunol.* **117:**1356–1362.
39. REGGIO, H. A., and J. C. DAGORN. 1978. Ionic interactions between bovine chymotrypsinogen A and chondroitin sulfate A.B.C. A possible model for molecular aggregation in zymogen granules. *J. Cell Biol.* **78:** 951–957.
40. REGGIO, H. A., and G. E. PALADE. 1978. Sulfated compounds in the zymogen granules of the guinea pig pancreas. *J. Cell Biol.* **77:**288–314.
41. REYNOLDS, E. S. 1963. The use of lead citrate at high pH as an electron opaque stain in electron microscopy. *J. Cell Biol.* **17:**208–212.
42. ROHLICH, P., P. ANDERSON, and B. UVNÄS. 1971. Electron microscopic observations on compound 48/80-induced degranulation in rat mast cells. *J. Cell Biol.* **51:**465–483.
43. TROTTER, C. M., and T. S. C. ORR. 1973. A fine structure study of some cellular components in allergic reactions. I. Degranulation of human mast cells in allergic asthma and perennial rhinitis. *Clin. Allergy.* **3:**411–425.
44. TROTTER, C. M., and T. S. C. ORR. 1974. A fine structure study of some cellular components in allergic reactions. II. Mast cells in normal and atopic human skin. *Clin. Allergy.* **4:**421–433.
45. WEINSTOCK, A., and J. T. ALBRIGHT. 1967. The fine structure of mast cells in normal human gingiva. *J. Ultrastruct. Res.* **17:**245–256.
46. YURT, R., and K. F. AUSTEN. 1977. Preparative purification of the rat mast cell chymase. Characterization and interaction with granule components. *J. Exp. Med.* **146:**1405–1419.
47. YURT, R. W., R. W. LEID, J. SPRAGG, and K. F. AUSTEN. 1977. Immunologic release of heparin from purified rat peritoneal mast cells. *J. Immunol.* **118:**1201–1207.